International Journal of Nanomedicine

Dovepress
open access to scientific and medical research

Open Access Full Text Article

ORIGINAL RESEARCH

A novel nano-copper-bearing stainless steel with reduced Cu^{2+} release only inducing transient foreign body reaction via affecting the activity of NF-κB and Caspase 3

This article was published in the following Dove Press journal:
International Journal of Nanomedicine
29 October 2015
Number of times this article has been viewed

Lei Wang[1,*]
Ling Ren[2,*]
Tingting Tang[1]
Kerong Dai[1]
Ke Yang[2]
Yongqiang Hao[1]

[1]Shanghai Key Laboratory of Orthopaedic Implants, Department of Orthopaedics, Shanghai Ninth People's Hospital, Shanghai JiaoTong University School of Medicine, Shanghai, People's Republic of China; [2]Institute of Metal Research, Chinese Academy of Sciences, Shenyang, People's Republic of China

*These authors contributed equally to this work

International Journal of Nanomedicine downloaded from https://www.dovepress.com/
For personal use only.

Abstract: Foreign body reaction induced by biomaterials is a serious problem in clinical applications. Although 317L-Cu stainless steel (317L-Cu SS) is a new type of implant material with antibacterial ability and osteogenic property, the foreign body reaction level still needs to be assessed due to its Cu^{2+} releasing property. For this purpose, two macrophage cell lines were selected to detect cellular proliferation, apoptosis, mobility, and the secretions of inflammatory cytokines with the influence of 317L-Cu SS. Our results indicated that 317L-Cu SS had no obvious effect on the proliferation and apoptosis of macrophages; however, it significantly increased cellular migration and TNF-α secretion. Then, C57 mice were used to assess foreign body reaction induced by 317L-Cu SS. We observed significantly enhanced recruitment of inflammatory cells (primarily macrophages) with increased TNF-α secretion and apoptosis level in tissues around the materials in the early stage of implantation. With tissue healing, both inflammation and apoptosis significantly decreased. Further, we discovered that NF-κB pathway and Caspase 3 played important roles in 317L-Cu SS induced inflammation and apoptosis. We concluded that 317L-Cu SS could briefly promote the inflammation and apoptosis of surrounding tissues by regulating the activity of NF-κB pathway and Caspase 3. All these discoveries demonstrated that 317L-Cu SS has a great potential for clinical application.

Keywords: nano-copper, foreign body reaction, inflammation, apoptosis, NF-κB, Caspase 3

Introduction

The clinical application of implant materials in orthopedic surgery has a long history, which enables the patients to have improved characteristics such as fracture healing, bone defects repair, and limb function. Currently, the primary implant material used in orthopedic surgery is generally a kind of metal, such as stainless steel (SS) and titanium alloy. As established by experience from its clinical use for bone replacement, both SS and titanium alloys have a good biocompatibility, excellent mechanical strength, and satisfactory corrosion resistance in vivo. However, these implants can only be termed "mechanical implants" because they lack essential biological properties, such as anti-microbial or osteogenic ability. Therefore, many researchers have performed a lot of studies to improve the biological properties of SS or titanium alloy, including increasing biological coating or adding biological elements,[1–6] and have achieved significant progress.

However, most of the implants currently used cannot fully meet their intended purpose because of severe inflammatory response and cytotoxicity. Therefore, in addition to good physical, chemical, and mechanical characteristics, the implants first must

Correspondence: Yongqiang Hao
Shanghai Key Laboratory of Orthopaedic Implants, Department of Orthopaedics, Shanghai Ninth People's Hospital, Shanghai JiaoTong University School of Medicine, Shanghai JiaoTong University, 639 Zhizaoju Road, Shanghai 200011, People's Republic of China
Tel +86 21 2327 1699
Fax +86 21 6313 6856
Email hyq_9hospital@hotmail.com

Ke Yang
Institute of Metal Research, Chinese Academy of Sciences, 72 Wenhua Road, Shenyang 110016, People's Republic of China
Tel +86 24 2397 1880
Fax +86 24 2397 1880
Email kyang@imr.ac.cn

© 2015 Wang et al. This work is published by Dove Medical Press Limited, and licensed under Creative Commons Attribution – Non Commercial (unported, v3.0) License. The full terms of the License are available at http://creativecommons.org/licenses/by-nc/3.0/. Non-commercial uses of the work are permitted without any further permission from Dove Medical Press Limited, provided the work is properly attributed. Permissions beyond the scope of the License are administered by Dove Medical Press Limited. Information on how to request permission may be found at: http://www.dovepress.com/permissions.php

possess a sufficient level of biocompatibility. In detail, all of the biomaterials for hosts belong to a foreign body, which is bound to cause a certain degree of foreign body reaction (FBR). FBR is a inevitable complicated and dynamic inflammatory process that may result in the immunological reactions originating from both injured tissues and the presence of a grafted biomaterial or an implant.[7] In this environment, macrophages, lymphocytes, and mast cells will infiltrate into the implant's surrounding area, and foreign body giant cells (multinucleated fused macrophages) and a dense fibrotic connective tissue layer will subsequently form and remain, which is detrimental to the implant's function, safety, and biocompatibility.[8–10] Therefore, only if the FBR does not exceed the capacity of the host or can be eliminated, can the implant be expected to be used in clinical applications.

Copper is one of the indispensable elements in the human body. An abnormal level of Cu in the body is always associated with a variety of diseases. For example, Cu deficiency can cause neurodegeneration[11] and cardiovascular disorders,[12] whereas Cu overload may be accompanied with hepatic and neurological diseases.[13,14] Nevertheless, Cu has been widely used in female intrauterine devices as an implant material[15] which can effectively disturb the fertilization process or zygote cots through the sperm cytotoxicity of Cu ions or worsening of the endometrial inflammatory response. Cu was determined to provide good antibacterial properties[16,17] and osteogenic properties[18,19] which has prompted many researchers to make an effort to add Cu into the orthopedic implant materials in anticipation of achieving some improved biological activities. Some scholars attempted to add a Cu coating onto the surface of orthopedic implants through different processing techniques.[20,21] However, the coating technique might lead to a massive release of Cu ions or tiny Cu particles, which would cause a relatively severe and persistent FBR in vivo.[7] Therefore, determining how to reduce the cytotoxicity and pro-inflammatory properties of Cu is the prerequisite for its use in clinical applications. Different from the previous coating technique, we developed a novel bio-functional metallic biomaterial, namely, Cu-bearing SS, in which about 4.5 weight percentage of nano-Cu was directly added to the conventional medical SS, such as 304, 316L, and 317L SS, during the steel making process. Such Cu-bearing SS has been demonstrated to possess strong antibacterial properties and certain osteogenic properties[6,22–24] without sacrificing the original mechanical strength and corrosion resistance. However, it was measured that about 1.4 ppb/day/cm^2 of Cu^{2+} ions could be released from Cu-bearing SS in short-term observation (0 to 30 days) in our previous study.[6] Due to the potential pro-inflammatory and cytotoxic abilities of Cu^{2+} ions, the focus will be on assessing the extent of the FBR caused by this new material through in vitro and in vivo experiments, including the influence of 317L-Cu SS on the proliferation, apoptosis, migration, and inflammatory cytokine secretion of inflammatory cells; the systemic toxicity potential; and the degree and duration of local FBR. Additionally, the activities of the key inflammation regulator NF-κB signaling pathway and the apoptosis executioner Caspase 3 will be detected, which is beneficial for finding effective methods to further reduce the FBR and enhance biocompatibility.

Materials and methods

Implant materials and characteristics detection

Implant materials production

317L-Cu SS was designed and fabricated by the Institute of Metal Research, Chinese Academy of Sciences, Shenyang, People's Republic of China. The nominal chemical compositions of 317L-Cu SS are Fe-19Cr-14Ni-3Mo-4.5Cu in weight percentage and the detailed production process was mentioned in our previous study.[6] Samples were cut into small round disks of two sizes: 1) larger disk of 10 mm in diameter and 1 mm in thickness was only used for in vitro experiments; 2) smaller disk of 5 mm in diameter and 1 mm in thickness was used for both in vitro and in vivo experiments. In addition, a medical grade 317L SS with the same sample shapes was used as the control material. These samples were mechanically polished with silicon carbide papers down to 2,000 grade and were ultrasonically washed in acetone and ethanol. All the samples were sterilized before performing the experiments involved in our study.

Metallurgical structures analysis by optical microscope (OM)

Microstructure was examined on Axiovert 200 MAT OM optical microscope, the samples for OM observations were prepared using the conventional metallographic procedure of grinding and mechanical polishing and then chemically etched in a solution composed of 5g $FeCl_3$ and 40 mL HCl.

Surface structure observation and elemental analysis by scanning electron microscopy (SEM) and energy dispersive spectroscopy (EDS) detection

Samples for SEM observation were carefully washed first. Subsequently, the samples were dried with graded alcohol. The surface microstructure of the samples was observed using

a scanning electron microscope (Joel JSM-6310LV, JEOL, Tokyo, Japan). Simultaneously, the metallic element type and proportion were detected by the EDS analysis technology.

Microstructure observation by X-ray diffraction (XRD) detection

In order to check whether Cu addition would alter the basic structure of SS, XRD technology was employed to characterize the structure of 317L-Cu SS. A D/max 2500 pc X-ray diffractometer (Rigaku, Tokyo, Japan) was used to analyze the variation in lattice constant of the experimental steel, with Cu-Kα radiation, tube voltage of 50 kV, tube current of 300 mA, and scanning speed of 1.2°/min.

Long-term analysis of Cu^{2+} ions released from 317L-Cu SS by inductively coupled plasma atomic emission spectroscopy

In order to quantitatively determine the amount of Cu^{2+} ions released from the 317L-Cu SS in a biological environment, the disc samples were immersed in physiological saline solution (0.9% NaCl solution with pH =7.4). The ten samples containing 3 mL of physiological saline solution were placed in a 37°C incubator for 5 days, 10 days, 20 days, 30 days, 40 days, 60 days, and 80 days, respectively. Afterward, an inductively coupled plasma atomic emission spectrometer (IRIS Intrepid; Thermo Fisher Scientific, Waltham, MA, USA) was used to quantify the amount of Cu^{2+} ions released from samples in the collected physiological saline solutions.

In vitro experiments

Cell culture

Mouse macrophage cell lines, Raw 264.7 and Ana-1 cells, were purchased from the Institute of Biochemistry and Cell Biology, Chinese Academy of Sciences, Shanghai, People's Republic of China. These lines were authenticated using DNA fingerprinting (variable number of tandem repeats), confirming that no cross-contamination occurred during this study. The cell lines were used within 6 months after resuscitation. Cells were grown in Minimum Essential Medium α (α-MEM) (Thermo Fisher Scientific) supplemented with 10% fetal bovine serum (Thermo Fisher Scientific) containing 100 U/mL penicillin, and 100 μg/mL streptomycin (Hyclone, Logan, UT, USA) in 37°C humidified atmosphere with 5% CO_2. The media were changed every 3 days until confluent.

Cell viability test by cell counting kit-8 (CCK8) assay

A CCK-8 (Dojindo, Kumamoto, Japan) was used in this experiment to quantitatively evaluate the macrophage cell viability under the influence of the 317L-Cu SS. In detail, the smaller disks were first put into some 96-well plates, and then approximately 5×10^3 cells were seeded on each 317L-Cu SS disk. Cells were cultured in the above medium and conditions for 1, 3, 5, and 7 days. The culture medium was removed before CCK-8 examination. Subsequently, 100 μL of α-MEM medium and 10 μL of CCK-8 solution were added to each sample, followed by incubation at 37°C for 2.5 hours. The absorbance of CCK-8, which represents the cell viability, was detected at 450 nm using a microplate reader (BioTek, Winooski, VT, USA).

Apoptosis detection by flow cytometry

The larger disks were used in this part of the study to collect enough cells for apoptosis detection. Six 317L-Cu SS disks and 317L SS disks were simultaneously placed into a 24-well plate. Approximately 2×10^4 Raw 264.7 or Ana-1 cells were seeded onto each disk. The culture medium was exchanged to remove non-adherent cells after inoculation for 8 hours, while the adherent cells were left to continue to cultivate for 72 hours. Next, the cells on six 317L-Cu SS disks or 317L SS disks were collected for the flow cytometry apoptosis detection. Cells were treated in accordance with the instructions of the Vybrant® Apoptosis Assay Kit 2 (Thermo Fisher Scientific). Fluorescence activated cell sorting was performed using a FACScan flow cytometer (Beckman Coulter, Inc., Brea, CA, USA). Data were acquired using CELL Quest software to reveal the impact of 317L-Cu SS on cell apoptosis.

Cell migration test by transwell assay

The cell migration assay was performed using a 24-well Transwell chamber (Merck Millipore, Billerica, USA). The larger disks were placed on the bottom of the lower chamber, leaving approximately a 1 mm distance to the underside of the upper chamber. Next, 6×10^3 Raw 264.7 or Ana-1 cells were seeded in the upper chamber with an 8 μm pore. The lower chamber was filled with 500 μm of serum-free α-MEM. Six hours and 12 hours later, the migrated cells in the underside surface of the upper chamber were fixed with 4% paraformaldehyde/phosphate buffered saline (PBS) for 30 minutes at room temperature and stained with hematoxylin for dyeing. Finally, the images were acquired using an inverted light microscope (IX71; Olympus Corporation, Tokyo, Japan) with DP Controller software.

TNF-α and IL-10 secretion detection by enzyme-linked immunosorbent assay (ELISA)

The amounts of inflammatory cytokine TNF-α and anti-inflammatory cytokine IL-10 secreted into the medium, when

the macrophage cell lines were affected by the 317L-Cu SS, were determined using ELISA kits from RayBiotech (Norcross, GA, USA). First, the culture medium was collected and centrifuged at 10,000 rpm for 5 minutes to clear the remaining impurities and particles. Detection was performed according to the manufacturer's instructions, which was consecutively repeated three times. Finally, the mean values of triplicate samples were used to calculate the concentrations of TNF-α and IL-10 on the basis of a standard curve obtained with standard TNF-α and IL-10 provided from the kits.

In vivo experiments

Animals and surgical procedure

Experiments were performed in female C57BL/6J mice aged 10 weeks with an average body weight of 25.81±2.7 g (Shanghai Sipper BK Laboratory Animals Ltd, Shanghai, People's Republic of China). The mice were kept in a barrier facility under high-efficiency particulate air filtration and allowed ad libitum access to water and standard laboratory pellets. The anesthetic, surgical, and postoperative care procedures followed the protocols approved by the local animal ethics committee at Shanghai JiaoTong University.

Mice were anesthetized with 1% sodium pentobarbital (40 mg/kg) by intraperitoneal injection on a clean bench. The surgical sites were first shaved, followed by alcohol disinfection and skin incision by blunt dissection of the subcutaneous tissue. Next, the implants were carefully placed into small pockets in the femoral musculature, and then these pockets and skin wounds were sutured with a suitable non-resorbable medical thread layer by layer. No antibiotic treatment was used before, during, or after the implantation. At 3 days, 1 week, 2 weeks, and 3 weeks post-surgery, six mice in each group were sacrificed for the subsequent experiments.

Serum Cu^{2+} detection by Cu^{2+} ions chromogenic reaction

Blood was collected into procoagulant tubes by enucleation and then centrifuged at 4,000 rpm for 10 minutes after the blood coagulation and clot contraction. Subsequently, the supernatant was transferred to new centrifuge tubes for detecting the concentration of Cu^{2+}, which was performed according to the instructions of QuantiChrom™ Copper Assay Kit (BioAssay Systems, Hayward, CA, USA).

Histological observation of liver and local muscle tissues by hematoxylin and eosin staining

The liver and muscle tissues surrounding the materials were dissected and harvested at each time point. These tissues were fixed in 4% paraformaldehyde/PBS overnight at 4°C, followed by dehydration in an ethanol series (75%, 80%, 85%, 90%, 95%, and 100%) and then embedding in paraffin. Subsequently, the tissues were serially cut into 5 μm thick sections, which were then deparaffinized and stained with hematoxylin and eosin. Histological observation was performed using a light microscope.

Qualitative and/or semi-quantitative analysis of inflammatory cells, local tissue TNF-α secretion detection, and Caspase 3 activity assay by immunohistochemistry

Immunohistochemical staining was performed on 5 μm thick formalin-fixed paraffin embedded sections. Deparaffinization was performed in xylene, while rehydration was performed in an ethanol series (100%–50%). Sections were then treated with H_2O_2 solution (3% H_2O_2 in PBS buffer) for 30 minutes to block endogenous peroxidase. Retrieval buffer (pH =9.0, Tris(hydroxymethyl)aminomethane 20 mmol/L, ethylenediaminetetraacetic acid 0.05 mmol/L, 0.05% Tween 20) was used for antigen retrieval in a 99°C bath for 20 minutes. Subsequently, primary antibodies: anti-CD3 (diluted 1:100 [abcam, Cambridge, MA, USA]), anti-CD68 (diluted 1:100 [abcam]), anti-CD163(diluted 1:100 [Bioss, Beijing, People's Republic of China]), anti-TNF-α (diluted 1:100, BioWorld, Visalia, CA, USA), and anti-cleaved-Caspase 3 (diluted 1:100, Cell Signaling Technology, Danvers, MA, USA) were applied to the sections, which were then incubated at 4°C overnight. After rinsing with the PBS buffer, the secondary antibody (MaxVision TM HRP-Polymer anti-Rabbit IHC Kit; Maixin. Bio, Fuzhou, People's Republic of China) was applied for 15 minutes at room temperature. 3,3′-Diaminobenzidine (Maixin. Bio) solution was used as chromogen. Finally, the sections were counterstained with hematoxylin (Sigma-Aldrich Co., St Louis, MO, USA) to identify the nuclei. Observation was performed using a microscope (Leica DM 4000B; Leica Microsystems, Wetzlar, Germany) with BioQuant OSTEO II software (BioQuant Image Analysis Corporation, Nashville, TN, USA).

Detection of NF-κB signaling pathway activity by electrophoretic mobility shift assay (EMSA)

Nuclear extracts were extracted from the tissues surrounding the implants using NE-PER® Nuclear and Cytoplasmic Extraction Reagents (Thermo Fisher Scientific) according to the manufacturer's instructions. EMSA was performed using a non-radioactive NF-κB EMSA kit, following the manufacturer's instructions (Thermo Fisher Scientific). The sequence of the NF-κB probe was 5′-AGTTGAGGGGACTTTCCCAGGC-3′. Biotins were labeled in the 5′ end oligonucleotide. Crude

nuclear protein (15 mg) was incubated for 20 minutes at room temperature in a 15 μL binding reaction system, including: 1.5 μL of 10× binding buffer, 1.5 μL of poly(deoxyinosinic-deoxycytidylic) (1.0 μg/μL), and ddH_2O for a final volume of 10 μL. Next, 0.6 μL of Bio-NF-κB probe or Bio-mutant-NF-κB probe (500 fM) was added, and then the reaction was incubated for 20 minutes at room temperature. Where indicated, 1 μL and 2 μL of specific competitor cold oligonucleotide was added in 50× and 100× competing systems, respectively, before the probe labeling, and then incubated for 20 minutes. Protein-DNA complexes were resolved by electrophoresis at 4°C on a 6.5% acrylamide gel and subjected to autoradiography. Electrophoresis was performed on a 6.5% non-denaturing polyacrylamide gel at 175 V in 0.25× Tris(hydroxymethyl)-aminomethane-Boric acid-EDTA buffer (TBE) at 4°C for 1 hour. Gels were transferred to the banding membrane at 394 mA in 0.5× TBE at room temperature for 40 minutes. Next, crosslinking of the membrane was performed in a UV crosslink apparatus for 10 minutes (Immobilization) followed by blocking, streptavidin-horseradish peroxidase labeling, washing, and equilibration of the membrane, and obtaining the pictures through the Imager apparatus (Protein Simple, San Jose, CA, USA).

In situ cell death detection by terminal deoxynucleotidyl transferase 2′-deoxyuridine 5′-triphosphate nick end labeling (TUNEL) assay

The sections were routinely deparaffinized and rehydrated in accordance with the above procedure. Proteinase K (20 μg/mL, diluted in Tris(hydroxymethyl)aminomethane/HCl, pH 7.4) was used for tissue repair at room temperature for 20 minutes. Subsequently, sections were washed with PBS buffer and incubated with TUNEL reaction mixture for 60 minutes at 37°C in a dark place. Finally, fluorescence images were acquired by using a microscope (Leica DM 4000B) with BioQuant OSTEO II software.

Expression and activity analysis of Caspase 3 by Western blot

Cytoplasmic protein was prepared from the tissues surrounding the implants using NE-PER® Nuclear and Cytoplasmic Extraction Reagents according to the manufacturer's instructions. Ten percent sodium dodecyl sulfate polyacrylamide gel electrophoresis (SDS-PAGE) for pro-Caspase 3 and 15% SDS-PAGE for cleaved-Caspase 3 were used for protein electrophoresis. Different samples with an equal amount of protein were subjected to SDS-PAGE and then transferred to 0.22 μm polyvinylidene fluoride (PVDF) membranes, which were then blocked with 5% free fat milk at room temperature for 1 hour and subsequently incubated with anti-pro-Caspase 3/cleaved-Caspase 3 primary antibody (diluted 1:1,000, Cell Signaling Technology) overnight at 4°C. The next day, PVDF membranes were first washed with Tris-Buffered-Saline-Tween buffer and then incubated with a fluorescent secondary antibody purchased from LI-COR (Lincoln, NE, USA) in a dark place for 1 hour at room temperature. Finally, the signals were detected using an Odyssey two-color infrared fluorescence image system (LI-COR). Positive immunoreactive bands were quantified densitometrically, and normalized by GAPDH.

Statistical analysis

Each sample was analyzed in triplicate, and the experiments were repeated three times. All of the results were expressed as the mean ± standard error with n. Mean, standard deviation, and *P*-values based on the 2-tailed *t*-test were calculated with Excel (Microsoft Corporation, Redmond, WA, USA). $P<0.05$ was considered to be statistically significant.

Results

317L-Cu SS showed no difference in structure from 317L SS but could continuously release trace amounts of Cu^{2+}

The nano-copper particles added into the 317L SS matrix (317L-Cu SS) were clearly seen in the SEM results (Figure 1A). EDS analysis further proved that the construction of the new copper-bearing SS was successful (Figure 1B). In microstructure, there was no difference between 317L and 317L-Cu SS as shown in metallographic graphs (Figure 1C), and both of them are normal austenitic microstructures, indicating that the immobilization of Cu in the matrix of 317L SS would not affect the microstructure. Furthermore, from the XRD patterns of 317L SS and 317L-Cu SS shown in Figure 1D, it could be seen that there was no difference between the characteristic peaks of 317L SS and 317L-Cu SS. Both of the samples presented the normal austenitic structure, which demonstrated that addition of Cu would not affect the basic microstructure of SS. Interestingly, Figure 1E showed that trace amounts (0.137 ng/cm^2/day) of Cu^{2+} could be continuously released for a long time.

317L-Cu SS enhanced the migration of macrophage cell lines

To verify the influence of 317L-Cu SS on the proliferation, apoptosis, and migration of inflammatory cells, two macrophage cell lines, Raw 264.7 and Ana-1, were analyzed in vitro. CCK8 assay revealed that 317L-Cu SS had no consistent and significant impact on the proliferation

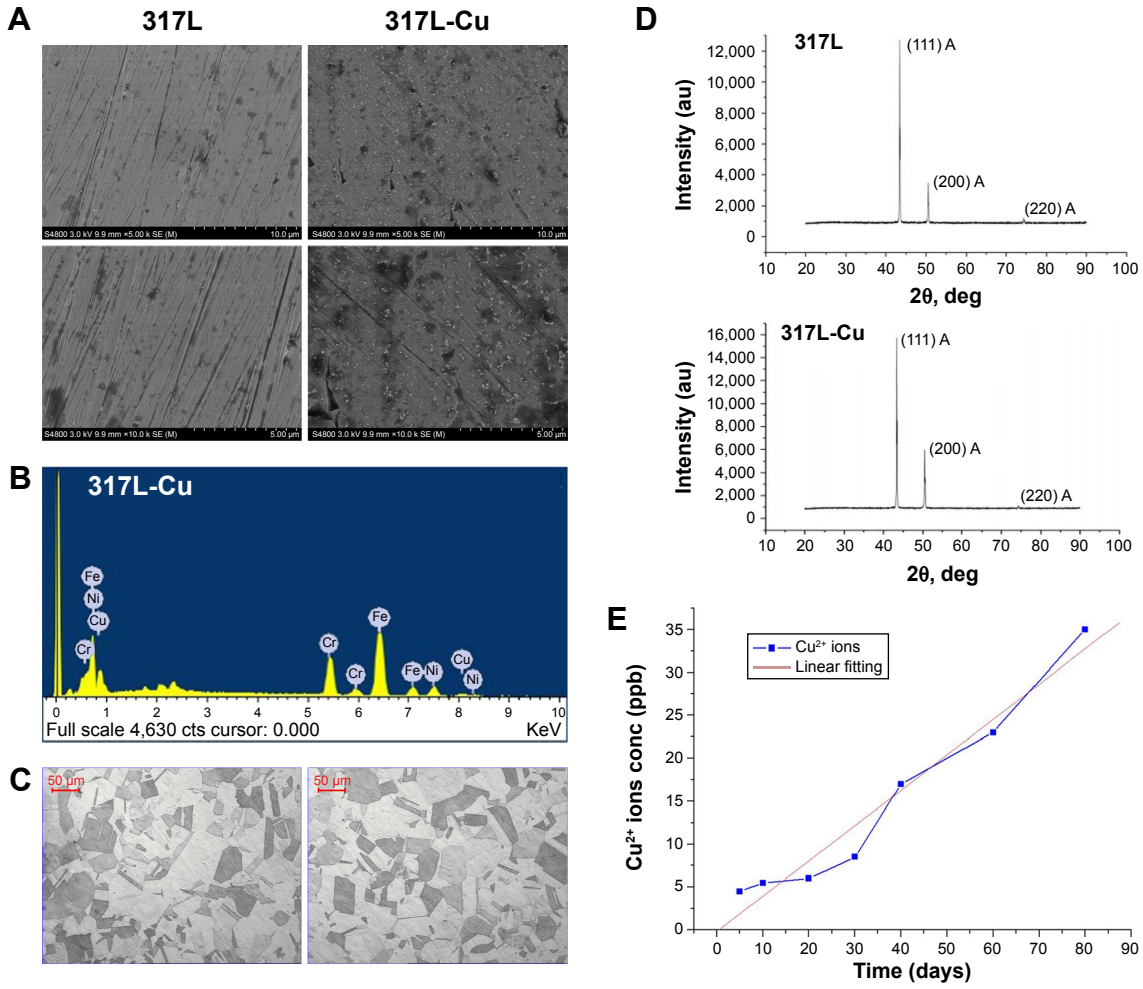

Figure 1 Characteristics observation of 317L-Cu SS.

Notes: Results of SEM and EDS proved the successful addition of nano-copper particles into the 317L SS matrix, in which nano-copper particles exhibited diffuse distribution (**A** and **B**). Both optical microscope observation and X-ray diffraction detection demonstrated that the addition of nano-copper particles did not change the microstructure of 317L-Cu SS compared to the 317L SS (**C** and **D**) (In **D**, "111", "200", "220" means indices of crystal face, while "A" means austenite structure of stainless steel). However, a relatively constant amount of Cu^{2+} was released from 317L-Cu SS every day, which would continue for a long time (**E**).

Abbreviations: au, arbitrary units; conc, concentration; cts, counts; deg, degrees; EDS, energy dispersive spectroscopy; SEM, scanning electron microscopy; SS, stainless steel.

of macrophage cells compared to 317L SS (Figure 2A). Seventy-two hour flow cytometry results indicated that cells on 317L-Cu SS exhibited a slightly higher apoptosis level (Raw 264.7 1.4% and Ana-1 3.64%) than those on 317L SS (Raw 264.7 0.39% and Ana-1 1.1%) with *P*-values of Raw 264.7>0.05 and Ana-1<0.05 (Figure 2B). However, the migration of both Raw 254.7 and Ana-1 was significantly enhanced when these cells were subjected to 317L-Cu SS for 6 hours and 12 hours (Figure 2C and D, respectively). These results demonstrated that 317L-Cu SS might have a strong inflammatory cell chemotactic effect but little effect on the proliferation and apoptosis.

317L-Cu SS promoted the secretion of TNF-α from macrophages

TNF-α, primarily generated by macrophages and monocytes, is a class of endogenous polypeptide with many powerful biological effects, including mediating a variety of immune responses. In the process of inflammation, TNF-α cannot only activate other inflammatory cells, such as neutrophils and lymphocytes, but also promote the synthesis and release of other cytokines. To understand the effect of 317L-Cu SS on the secretion of TNF-α from macrophages, we collected the supernatants of Raw 264.7 and Ana-1 cells to detect the level of TNF-α by ELISA assay. Cells on 317L-Cu SS were found to secrete more TNF-α than the control group. More specifically, Raw 264.7 cells on 317L-Cu SS responded more quickly, with a significant increased secretion of TNF-α, when incubated for 6 hours compared to Ana-1 cells, which exhibited high secretion of TNF-α until stimulation by 317L-Cu SS for 12 hours (Figure 3A and B). In addition, we examined the level of IL-10, one of the most important anti-inflammatory cytokines, in the macrophage supernatants. However, the level of IL-10 had no obvious

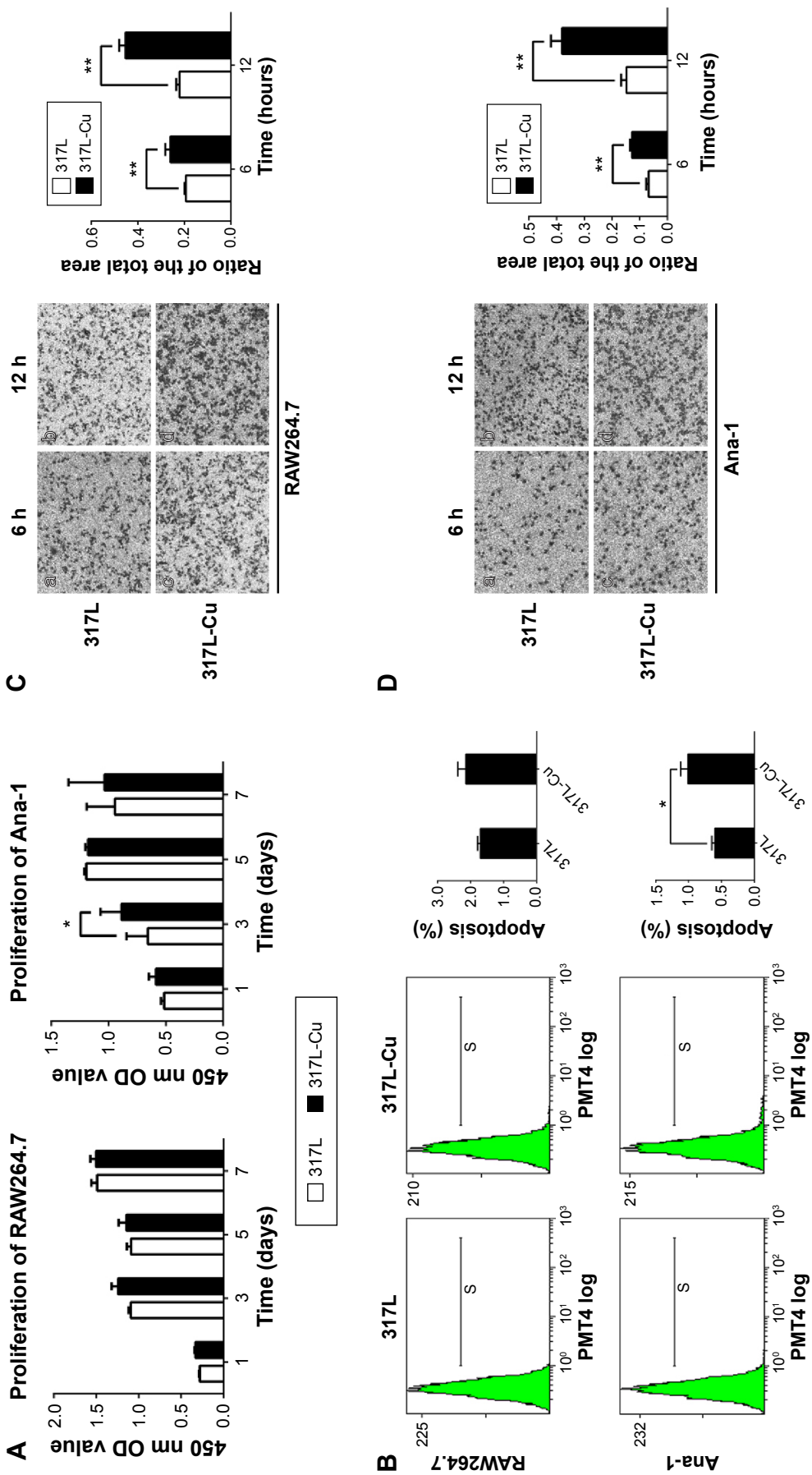

Figure 2 317L-Cu SS promoted the migration of macrophages without significant influence on cell proliferation and apoptosis.
Notes: CCK8 assay revealed that the proliferation of macrophages on the 317L-Cu SS had no significant difference compared to the control group (**A**). Both Raw 264.7 and Ana-1 cells under the influence of 317L-Cu SS for 72 hours showed a slightly higher apoptosis level, but the difference was not very significant (**B**). (PMT4 is the name of the channel for annexin V positive cells in our flow cytometry instrument. "S" is just a tag for positive area). However, in the grayscale images (**C** and **D**), migrated cells were black-stained. To the naked eye view, more black-stained migratory cells were observed in 317L-Cu SS group in 6 hours and 12 hours (**c** and **d**) than 317L SS group (**a** and **b**), indicating that 317L-Cu SS possessed stronger macrophage-induced ability than 317L SS. The ratio of migrated cells area to the total view area was used to calculate the statistical differences between groups. $^{*}P<0.05$, $^{**}P<0.01$.
Abbreviations: SS, stainless steel; CCK8, cell counting kit-8; h, hours; OD, optical density.

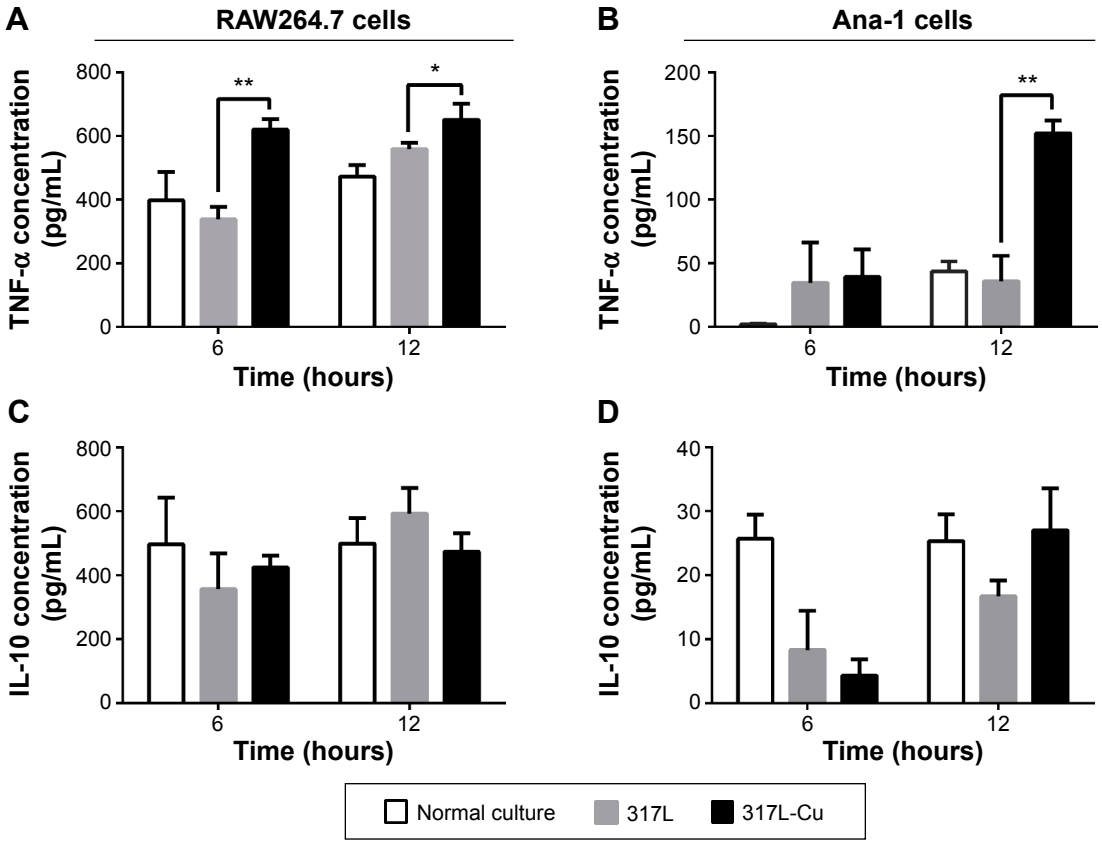

Figure 3 317L-Cu SS effectively increased TNF-α secretion in vitro.
Notes: Higher TNF-α secretion in two cell lines in the 317L-Cu SS group was detected by ELISA. Specially, Raw 264.7 cells exhibited faster response to 317L-Cu SS than Ana-1 cells, ie, the significantly increased secretion of TNF-α in Raw 264.7 cells could be detected in 6 hours, while Ana-1 cells needed 12 hours (**A** and **B**). Simultaneously, IL-10, a key anti-inflammatory cytokine, was also analyzed. Unfortunately, IL-10 secretion did not show any consistent and significant changes in the two cells when incubated on 317L-Cu SS and 317L SS (**C** and **D**). *$P<0.05$, **$P<0.01$.
Abbreviations: SS, stainless steel; ELISA, enzyme-linked immunosorbent assay.

and consistent changes in the two cell lines (Figure 3C and D). Collectively, these results suggested that 317L-Cu SS might have some effects on promoting the secretion of inflammatory cytokines.

317L-Cu SS should have no systemic toxicity in vivo

Animal models were used to further clarify the effects of 317L-Cu SS on the characteristics of macrophages' in vivo environment. Serum Cu^{2+} concentration and hepatic pathology were first detected. The results revealed that there was no significant difference in serum Cu^{2+} concentration between the 317L-Cu SS group and the 317L SS group at 3 days, 1 week, 2 weeks, and 3 weeks after modeling (Figure 4A). Meanwhile, hepatic pathological changes of the 317L-Cu SS group were also not found in the histological specimens (Figure 4B). Thus, it was proven that 317L-Cu SS did not release any copper ions into serum to cause further injury to other organs in vivo.

317L-Cu SS increased local infiltration of inflammatory cells only in the early stage

Implants surrounding tissue were collected to detect the extent of local FBR caused by 317L-Cu SS and 317L SS. Compared to 317L SS, 317L-Cu SS implants were covered by a relatively thicker connective tissue layer with a higher degree of inflammatory cells infiltration at 3 days and 1 week after implantation. However, with the development of tissue healing in 2 weeks and 3 weeks, the connective tissue layer was observed to become thinner and thinner, accompanied by substantial regression of inflammatory cells (Figure 5A). Further, the types of inflammatory cells were identified by immunohistochemistry staining: CD3 for lymphocytes, CD68 for macrophages and CD163 for monocytes and macrophages. Our results revealed that the infiltrated cells were mainly macrophages and monocytes and also contained a small amount of T lymphocytes in the early stage of inflammation. With the regression of inflammatory cells, the macrophages, monocytes, and T lymphocytes were significantly reduced in the connective

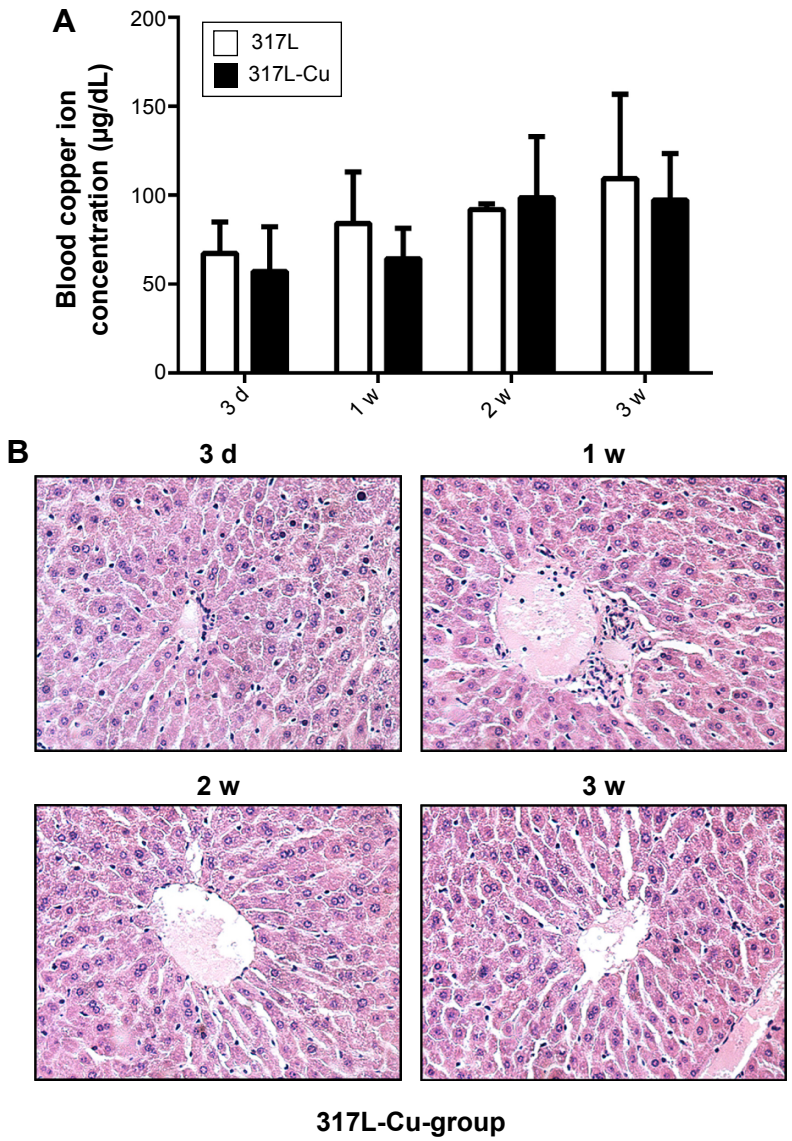

Figure 4 317L-Cu SS had no systemic toxicity.
Notes: No significant change of serum Cu^{2+} concentration was detected in the 317L-Cu SS group after implantation into the femoral musculature of C57BL/6J mice (**A**). Meanwhile, the liver, the main organ of Cu^{2+} metabolism, showed no obvious pathological changes in HE staining, and the indigo nuclei and red cytoplasm were divided (**B**).
Abbreviations: SS, stainless steel; HE, hematoxylin and eosin; d, days; w, week(s).

tissue layer (Figure 5B–D). Taken together, it was concluded that 317L-Cu SS could increase the local infiltration of inflammatory cells (mainly macrophages and monocytes) only in the early stage of implantation. With the passing of time, those infiltrated cells could significantly reduce, or even disappear.

317L-Cu SS promoted the secretion of TNF-α and further activated NF-κB signaling in the early stage of implantation

With a large number of inflammatory cells accumulated at 3 days and 1 week in vivo, increased secretion of TNF-α was detected in the 317L-Cu SS group. Meanwhile, TNF-α secretion in the 317L-Cu SS group significantly decreased in 2 weeks and 3 weeks after implantation, in agreement with the above results (Figure 6A). In view of the interaction between NF-κB and TNF-α as well as its important role in the modulation of inflammatory reaction, the activity of NF-κB was further evaluated by EMSA. The result indicated that the NF-κB signaling pathway was significantly up-regulated in the 317L-Cu SS group compared to the 317L SS group in the early stage of implantation (3 days and 1 week). However, at 2 weeks and 3 weeks, NF-κB activation of 317L-Cu SS group subsequently declined to almost no difference compared with the control group (Figure 6B). Therefore, we deduced that NF-κB might be a key signaling pathway for Cu^{2+} to regulate the inflammatory response in vivo.

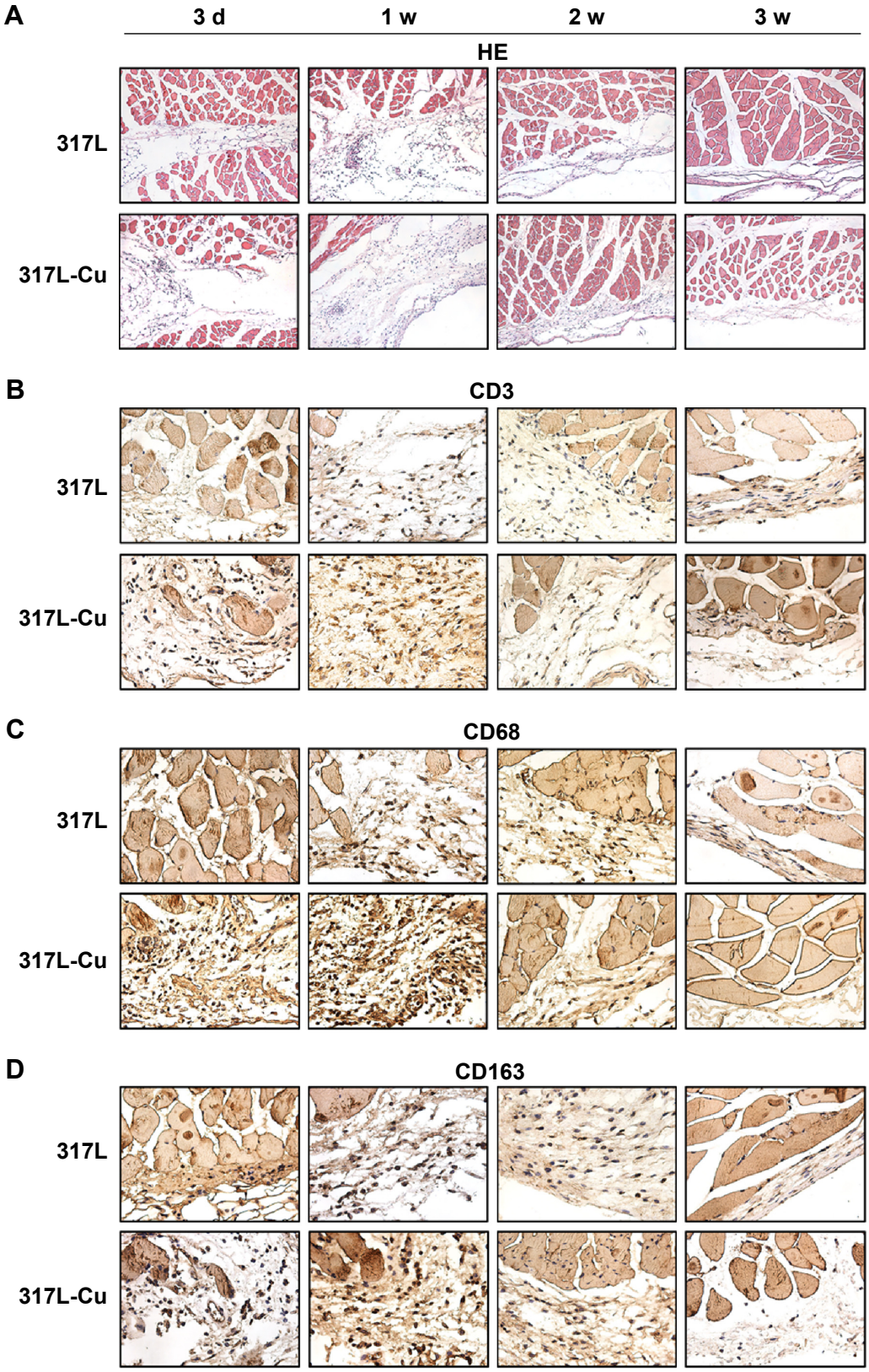

Figure 5 317L-Cu SS increased local infiltration of inflammatory cells (primarily macrophages) only in the early implantation stage.
Notes: HE staining revealed that a relatively thicker connective tissue layer (funicular and dyeing shallow) covered the 317L-Cu SS implants with a higher degree of inflammatory cells (indigo staining) infiltration at 3 days and 1 week after implantation. With the process of healing, the connective tissue layer and inflammatory cells were able to quickly reduce and even disappeared (**A**). By immunohistochemical identification of the cell types in which positive cells presented brown or black if there was overlap with the color of hematoxylin, it was found that the infiltrated inflammatory cells were mainly macrophages mixed with a small amount of T lymphocytes (**B**–**D**).
Abbreviations: SS, stainless steel; HE, hematoxylin and eosin; d, days; w, week(s).

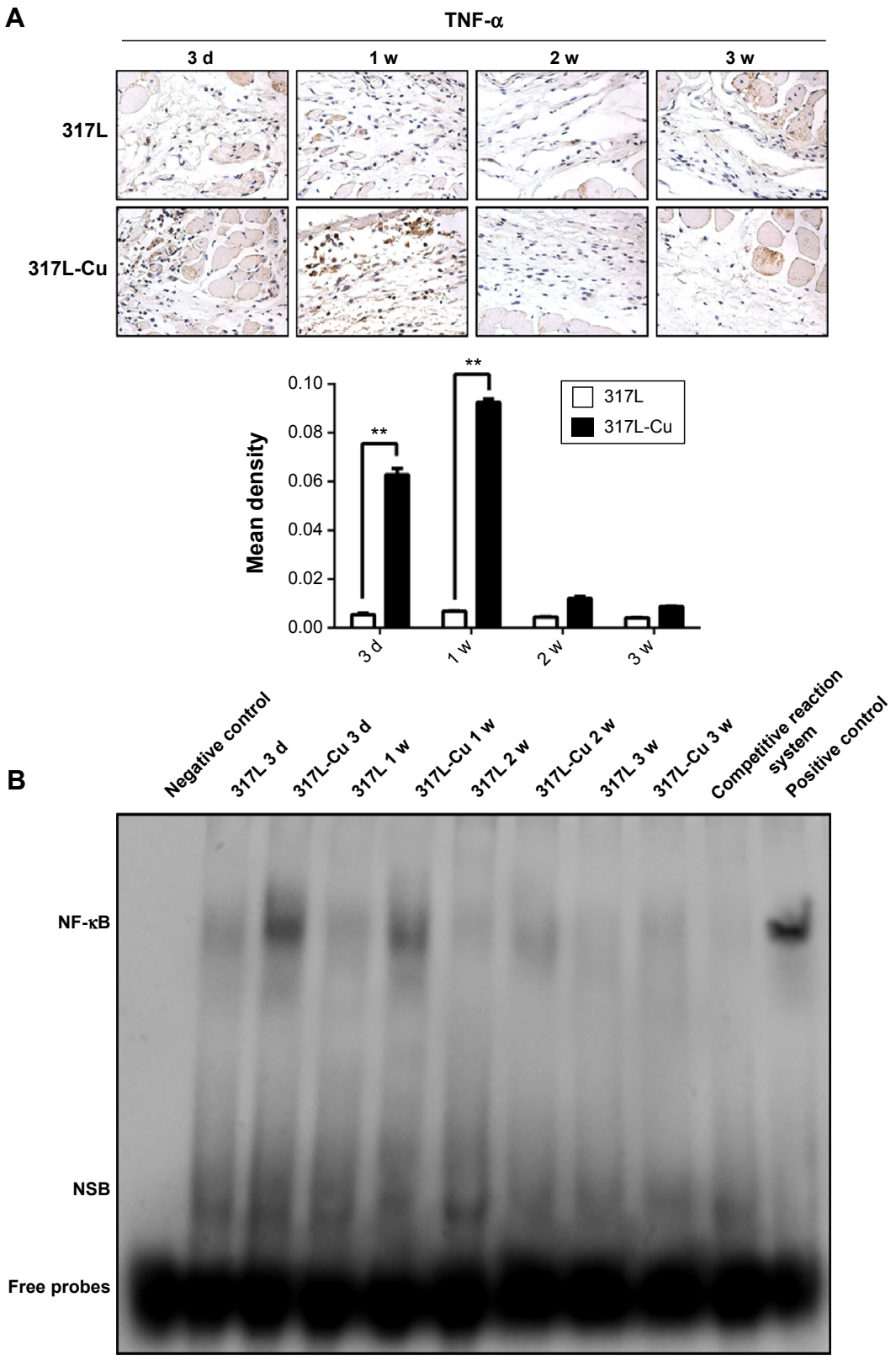

Figure 6 317L-Cu SS promoted TNF-α secretion accompanied by the activation of NF-κB signaling in the early stage of implantation.
Notes: Immunohistochemistry assay of material surrounding tissues revealed that 317L-Cu SS could cause more TNF-α secretion (brown staining indicated the positive area) at 3 days and 1 week after implantation. Similarly, the amount of TNF-α significantly decreased in 2 weeks and 3 weeks (**A**). EMSA results showed that the activity of NF-κB signaling pathway could be significantly up-regulated by 317L-Cu SS in the early stage of implantation. At 2 weeks and 3 weeks, its activity was substantially restored to normal status (**B**). $^{**}P<0.01$.
Abbreviations: SS, stainless steel; EMSA, electrophoretic mobility shift assay; NSB, Nonspecific Binding; d, days; w, week(s).

317L-Cu SS induced higher tissue apoptosis by up-regulating the activity of Caspase 3 in the early stage of implantation

Tissue apoptosis is also an important manifestation of FBR. Our TUNEL assay in vivo revealed that 317L-Cu SS induced more tissue apoptosis at 3 days and 1 week compared to 317L SS, which peaked at 1 week. The degree of tissue apoptosis gradually decreased and almost had no positive performance until 2 weeks and 3 weeks (Figure 7A). Tissue proteins were extracted to test the expression and activity of Caspase 3, which is a key regulator of apoptosis. Consistent with the TUNEL results, Western blot analysis indicated that the expression of pro-Caspase 3 was significantly up-regulated in 317L-Cu SS at 3 days and 1 week after implantation, which also peaked at 1 week. Generally, the overall trend of 317L-Cu SS initially increased and then decreased until no difference from the control group was observed. As expected, the variation tendency of cleaved-Caspase 3, ie, Caspase 3 activity, was basically consistent with the results of pro-Caspase 3 (Figure 7B). To further confirm the activity changes of Caspase 3, the expression of cleaved-Caspase 3 in tissue sections was detected again by immunohistochemistry staining, in which a relatively high level of cleaved-Caspase 3 was observed at 3 days, 1 week, and 2 weeks after implantation, but no difference was observed at 3 weeks (Figure 7C). Collectively, 317L-Cu SS might increase the apoptosis level of surrounding tissue by changing the activity of Caspase 3 in the early stage of implantation.

Discussion

Treatment of orthopedic disorders often requires the use of a variety of implants, which should have sufficient strength and preferably also have a certain biological activity. For this reason, many scholars around the world have been committed to the development of new orthopedic implant materials with improved functionality, such as better antibacterial properties and osteogenic performance. However, the extent of FBR induced by these new materials has attracted little attention. As is known, every type of implant material causes FBR to some degree. The FBR responses to orthopedic implant materials is often characterized by persistent and severe inflammatory reaction and increased tissue apoptosis, with the specific processes as follows: cytokines, chemokines, and other pro-inflammatory molecules are released at the implant interface by polymorphonuclear leukocytes, macrophages, activated fibroblasts, and other cells, thereby disturbing normal homeostatic mechanisms.[25] Even worse, if this process continues without resolution, it results in chronic inflammation and osteolysis, jeopardizing the long-term stability of the implant.[26] Therefore, we believe that an effective new implant material should have good biocompatibility with lower FBR induction.

317L-Cu SS is a new copper-containing SS for implantation, developed by the Institute of Metal Research, Chinese Academy of Sciences, with excellent antibacterial ability and osteogenic property as previously mentioned. Due to a certain release of Cu^{2+}, which can cause certain cytotoxicity and cell apoptosis,[27] the biocompatibility and FBR inducing ability of 317L-Cu SS should be carefully evaluated. In our study, we found that this new material was able to obviously induce the migration of macrophages, ie, stronger chemotaxis, without significant and consistent influence on their proliferation and apoptosis. In the early implantation stage, ie, 3 days and 1 week after implantation in the present study, there was a thicker connective tissue layer surrounding the 317L-Cu SS, in which considerable inflammatory cells (mainly macrophages) gathered with significantly increased secretion of TNF-α. Conversely, with the healing of tissue in the later implantation stage, the connective tissue layer became thinner, and the inflammatory cells as well as the inflammatory factors disappeared. All of these results had no significance compared to the control group. Thus, we suggested that a temporary stress reaction in vivo occurred in response to 317L-Cu SS implantation, which was manifested as the aggregation of inflammatory cells, further increasing the expression of inflammatory factors and the amount of apoptosis in tissue. However, these changes did not last for a long time, they were reduced and even disappeared, with the process of tissue healing.

Generally, the autologous immune response, induced by infection or trauma, is an important defense mechanism in the human body. However, the immune response is also the main cause of FBR to the implant materials in orthopedics. As is known, the occurrence (and even the extent) of inflammation is closely related to the activation of NF-κB pathway, which is mediated by various receptors located on the extra- and intra-cellular membranes. Many cytokines, such as TNF-α and IL-1,[28] can act in paracrine as well as autocrine manner to activate the NF-κB signaling pathway which subsequently promotes pro-inflammatory cytokines, chemokines, and adhesion molecules, acute phage proteins, inducible effector enzymes, regulators of cell proliferation and apoptosis.[29] Because of its functional significance associated with innate and adaptive immunity, it is deduced that the NF-κB pathway

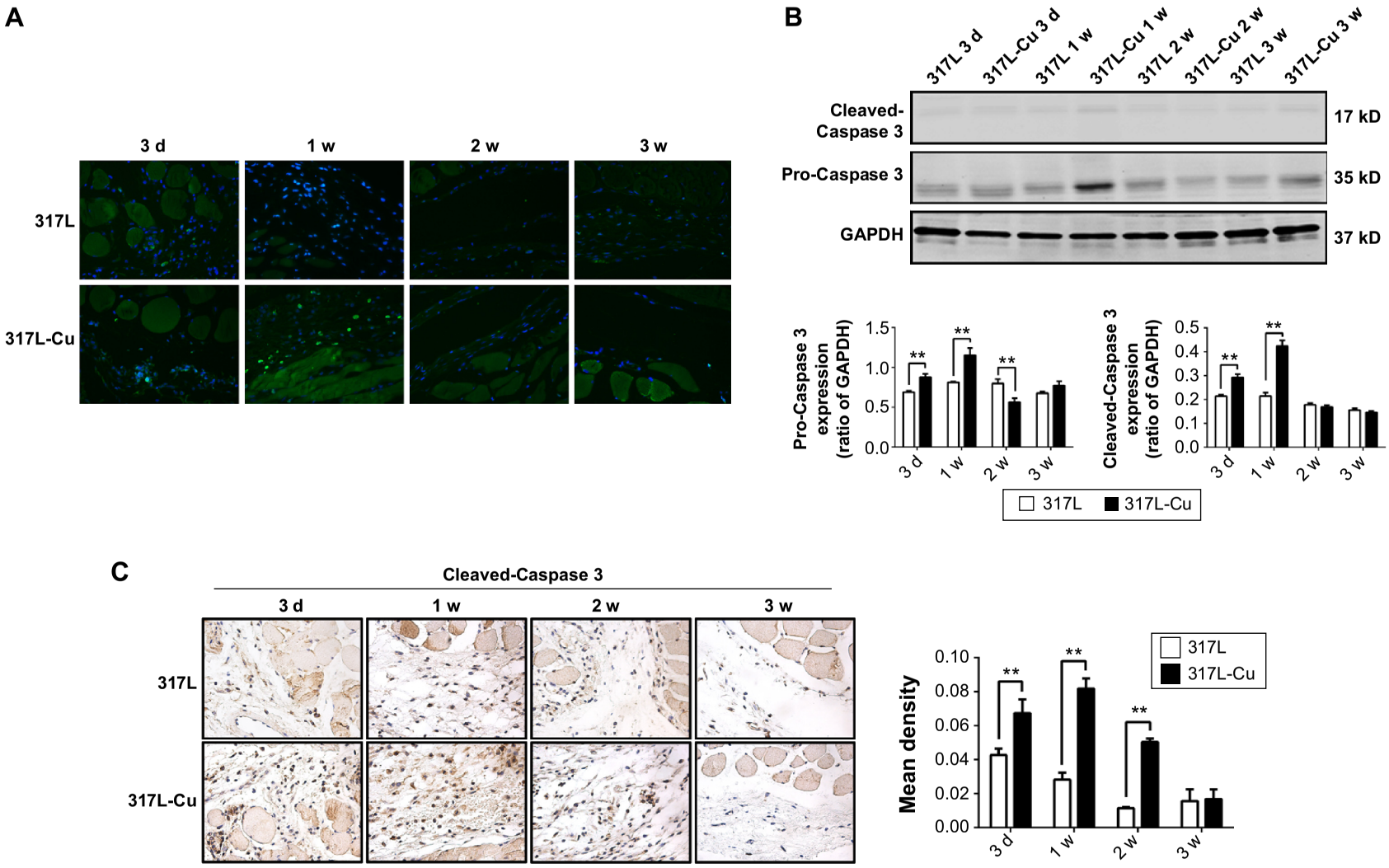

Figure 7 317L-Cu SS induced higher tissue apoptosis by up-regulating the activity of Caspase 3 in the early stage of implantation.

Notes: TUNEL assay revealed that there was more apoptotic tissue and cells around the 317L-Cu SS in the early stage of implantation. With the process of tissue healing, apoptotic tissue and cells were rapidly cleared in 2 weeks and 3 weeks after implantation (**A**). Western blot and immunohistochemistry demonstrated that apoptosis induced by 317L-Cu SS was most likely related to the expression and activity of Caspase 3, whose variation tendency was basically consistent with the macro apoptosis performance of tissues (**B** and **C**). Apoptotic tissues and cells showed green fluorescence in the TUNEL assay; positive staining for cleaved-Caspase 3 was brown or black in immunohistochemistry. $^{**}P<0.01$.

Abbreviations: SS, stainless steel; TUNEL, terminal deoxynucleotidyl transferase 2′-deoxyuridine 5′-triphosphate nick end labeling; d, days; w, week(s); GAPDH, glyceraldehyde-3-phosphate dehydrogenase.

might play an important role in regulating some biological behaviors of macrophages and lymphocytes.[30] In addition, some previous studies demonstrated that COMMD1, one of the most frequently studied members of copper ion metabolism gene domain protein family, could effectively restrain the activity of NF-κB,[31,32] thus hinting that copper metabolism disorder might affect the activity of NF-κB pathway. Therefore, we first considered whether the NF-κB pathway had a certain utility in the transient enhanced inflammation caused by such new copper-containing SS after being implanted into the body. The EMSA results indicated that the activity of NF-κB pathway first increased and then decreased, which was basically consistent with the trend of inflammatory cells' infiltration and TNF-α secretion. Consequently, we highly suspected that the released Cu^{2+} could effectively cause a transient activation of the NF-κB pathway in the surrounding tissues. Due to the limited amount and distribution of Cu^{2+} as well as the isolation effect of connective tissue, the NF-κB pathway could not be persistently activated in vivo. Apoptosis is often integrated with inflammation reaction, so the apoptotic level and the expression/activity of Caspase 3, the main regulatory factor for apoptosis,[33,34] was simultaneously evaluated. Our results indicated that the changes of Caspase 3 expression and activity were also first increased and later decreased in accordance with the trend of inflammation.

Macrophages participate in the healing process of many tissues and organs. Similarly, the initiation of fracture healing is also highly correlated with the early inflammatory reaction, regulating effects of macrophages.[35,36] Currently, many researchers are involved in studies of the effectiveness of macrophages on fracture healing. Xing et al[37] found that inhibiting the recruitment of inflammatory macrophages in fracture nonunion animal models led to decreased endochondral bone formation, but had no effect on the intramembranous bone formation. In addition, Alexander et al[38] also proposed a new viewpoint that bone-lining tissues contained a population of resident macrophages termed osteomacs, which were associated with intramembranous bone healing and were undertaking a pro-anabolic functional role unrelated to the ability to serve as an osteoclast precursor. Therefore, regarding the significant macrophages' recruitment ability of our new material, determining whether it can affect the fracture healing through regulating the biological behavior or functions of macrophages will be our emphasis of further research.

Conclusion

Taken together, our results confirmed that 317L-Cu SS had good biocompatibility, with a relatively low ability to induce FBR. Such a new material could briefly promote the inflammation reaction and apoptosis level of the surrounding tissues by regulating the activity of NF-κB pathway and Caspase 3, but these effects were not sustained. Therefore, the present results plus previous results of our team fully demonstrated that 317L-Cu SS possesses good antibacterial ability and osteogenic property, making it a new material with a considerable potential in clinical application.

Acknowledgments

This work was supported by grants from the Key National Basic Research Program of China (2012CB619101), the National Natural Science Foundation of China (numbers: 81071472, 81371960, and 81301329), the Industry-University-Research-Medical Cooperation Project of the Science and Technology Commission of Shanghai (12DZ1940203), the Technology Support Project of the Science and Technology Commission of Shanghai (13441901302 and 14441901000), the New Cutting-Edge Technology Project of ShenKang Hospital Development Center of Shanghai (SHDC12014124), and Doctoral Innovation Fund Projects from Shanghai Jiao Tong University School of Medicine (BXJ201429).

Disclosure

The authors report no known conflicts of interest associated with this publication and that there has been no significant financial support for this work that could have influenced its outcome.

References

1. Leitão E, Barbosa MA, de Groot K. Influence of substrate material and surface finishing on the morphology of the calcium-phosphate coating. *J Biomed Mater Res*. 1997;36(1):85–90.
2. Mustafa A, Lung CY, Mustafa NS, et al. EPA-coated titanium implants promote osteoconduction in white New Zealand rabbits. *Clin Oral Implants Res*. Epub 2014 Nov 13.
3. Fang K, Song W, Wang L, et al. Immobilization of chitosan film containing semaphorin 3A onto a microarc oxidized titanium implant surface via silane reaction to improve MG63 osteogenic differentiation. *Int J Nanomedicine*. 2014;9:4649–4657.
4. Jin G, Cao H, Qiao Y, Meng F, Zhu H, Liu X. Osteogenic activity and antibacterial effect of zinc ion implanted titanium. *Colloids Surf B Biointerfaces*. 2014;117:158–165.
5. Hass JL, Garrison EM, Wicher SA, et al. Synthetic osteogenic extracellular matrix formed by coated silicon dioxide nanosprings. *J Nanobiotechnology*. 2012;10:6.
6. Ren L, Wong HM, Yan CH, Yeung KW, Yang K. Osteogenic ability of Cu-bearing stainless steel. *J Biomed Mater Res B Appl Biomater*. Epub 2014 Nov 23.
7. Bartsch I, Willbold E, Yarmolenko S, Witte F. In vivo fluorescence imaging of apoptosis during foreign body response. *Biomaterials*. 2012;33(29):6926–6932.
8. Anderson JM, McNally AK. Biocompatibility of implants: lymphocyte/macrophage interactions. *Semin Immunopathol*. 2011;33(3):221–233.

9. Luttikhuizen DT, Harmsen MC, Van Luyn MJ. Cellular and molecular dynamics in the foreign body reaction. *Tissue Eng*. 2006;12(7):1955–1970.
10. Morais JM, Papadimitrakopoulos, Burgess DJ. Biomaterials/tissue interactions: possible solutions to overcome foreign body response. *AAPS J*. 2010;12(2):188–196.
11. Kumar N. Copper deficiency myelopathy (human swayback). *Mayo Clin Proc*. 2006;81(10):1371–1384.
12. Zhang S, Liu H, Amarsingh GV, et al. Diabetic cardiomyopathy is associated with defective myocellular copper regulation and both defects are rectified by divalent copper chelation. *Cardiovasc Diabetol*. 2014;13:100.
13. Cox DW, Moore SD. Copper transporting P-type ATPases and human disease. *J Bioenerg Biomembr*. 2002;34(5):333–338.
14. Desai V, Kaler S. Role of copper in human neurological disorders. *Am J Clin Nutr*. 2008;88(3):855S–858S.
15. Hubacher D, Lara-Ricalde R, Taylor DJ, Guerra-Infante F, Guzmán-Rodríguez R. Use of copper intrauterine devices and the risk of tubal infertility among nulligravid women. *N Engl J Med*. 2001;345(8):561–567.
16. Casey AL, Adams D, Karpanen TJ, et al. Role of copper in reducing hospital environment contamination. *J Hosp Infect*. 2010;74(1):72–77.
17. Salgado CD, Sepkowitz KA, John JF, et al. Copper surface reduce the rate of healthcare-acquired infections in the intensive care unit. *Infect Control Hosp Epidemiol*. 2013;34(5):479–486.
18. Wu C, Zhou Y, Xu M, et al. Copper-containing mesoporous bioactive glass scaffolds with multifunctional properties of angiogenesis capacity, osteostimulation and antibacterial activity. *Biomaterials*. 2013;34(2):422–433.
19. Rodríguez JP, Ríos S, González M. Modulation of the proliferation and differentiation of human mesenchymal stem cells by copper. *J Cell Biochem*. 2002;85(1):92–100.
20. Hoene A, Prinz C, Walschus U, et al. In vivo evaluation of copper release and acute local tissue reactions after implantation of copper-coated titanium implants in rats. *Biomed Mater*. 2013;8(3):035009.
21. Hoene A, Patrzyk M, Walschus U, et al. In vivo examination of the local inflammatory response after implantation of Ti6Al4V samples with a combined low-temperature plasma treatment using pulsed magnetron sputtering of copper and plasma-polymerized ethylenediamine. *J Mater Sci Mater Med*. 2013;24(3):761–771.
22. Ren L, Nan L, Yang K. Study of copper precipitation behavior in a Cu-bearing austenitic antibacterial stainless steel. *Mater Design*. 2011;32(4):2374–2379.
23. Ren L, Yang K. Bio-functional design for metal implants, a new concept for development of metallic biomaterials. *J Mater Sci Technol*. 2013;29(11):1005–1110.
24. Chai HW, Guo L, Wang XT, et al. Antibacterial effect of 317L stainless steel contained copper in prevention of implant-related infection in vitro and in vivo. *J Mater Sci Mater Med*. 2011;22(11):2525–2535.
25. Gallo J, Goodman SB, Konttinen YT, Raska M. Particle disease: Biologic mechanisms of periprosthetic osteolysis in total hip arthroplasty. *Innate Immun*. 2013;19(2):213–224.
26. Goodman SB, Yao Z, Keeney M, Yang F. The Future of Biologic Coatings for Orthopaedic Implants. *Biomaterials*. 2013;34(13):3174–3183.
27. Chung KC, Park JH, Kim CH, et al. Novel Biphasic Effect of Pyrrolidine Dithiocarbamate on Neuronal Cell Viability Is Mediated by the Differential Regulation of Intracellular Zinc and Copper Ion Levels, NF-kB, and MAP Kinases. *J Neurosci Res*. 2000;59(1):117–125.
28. Baldwin AS Jr. The NF-kB and IkB proteins: new discoveries and insights. *Ann Rev Immunol*. 1996;14:649–683.
29. Pal S, Bhattacharjee A, Ali A, Mandal NC, Mandal SC, Pal M. Chronic inflammation and cancer: potential chemoprevention through nuclear factor kappa B and p53 mutual antagonism. *J Inflamm (Lond)*. 2014;11:23.
30. Ghosh S, Karin M. Missing pieces in the NF-kappaB puzzle. *Cell*. 2002;109 Suppl:S81–S96.
31. Maine GN, Mao X, Komarck CM, Burstein E. COMMD1 promotes the ubiquitination of NF-kB subunits through a Cullin-containing ubiquitin ligase. *EMBO J*. 2007;26(2):436–447.
32. Li H, Chan L, Bartuzi P, et al. Copper Metabolism Domain-Containing 1 Represses Genes That Promote Inflammation and Protects Mice From Colitis and Colitis-Associated Cancer. *Gastroenterology*. 2014;147(1):184–195.e3.
33. Salvesen GS. Caspases and apoptosis. *Essays Biochem*. 2002;38:9–19.
34. Ried SJ, Shi Y. Molecular mechanisms of caspase regulation during apoptosis. *Nat Rev Mol Cell Biol*. 2004;5(11):897–907.
35. Einhorn TA, Majeska RJ, Rush EB, Levine PM, Horowitz MC. The expression of cytokine activity by fracture callus. *J Bone Miner Res*. 1995;10(8):1272–1281.
36. Gerstenfeld LC, Cullinane DM, Barnes GL, Graves DT, Einhorn TA. Fracture healing as a post-natal developmental process: molecular, spatial, and temporal aspects of its regulation. *J Cell Biochem*. 2003;88(5):873–884.
37. Xing Z, Lu C, Hu D, et al. Multiple roles for CCR2 during fracture healing. *Dis Model Mech*. 2010;3(7–8):451–458.
38. Alexander KA, Chang MK, Maylin ER, et al. Osteal Macrophages Promote In Vivo Intramembranous Bone Healing in a Mouse Tibial Injury Model. *J Bone Miner Res*. 2011;26(7):1517–1532.

International Journal of Nanomedicine

Dovepress

Publish your work in this journal

The International Journal of Nanomedicine is an international, peer-reviewed journal focusing on the application of nanotechnology in diagnostics, therapeutics, and drug delivery systems throughout the biomedical field. This journal is indexed on PubMed Central, MedLine, CAS, SciSearch®, Current Contents®/Clinical Medicine, Journal Citation Reports/Science Edition, EMBase, Scopus and the Elsevier Bibliographic databases. The manuscript management system is completely online and includes a very quick and fair peer-review system, which is all easy to use. Visit http://www.dovepress.com/testimonials.php to read real quotes from published authors.

Submit your manuscript here: http://www.dovepress.com/international-journal-of-nanomedicine-journal